Kent Academic Repository

Journal of
Materials Chemistry C

Materials for optical, magnetic and electronic devices

ROYAL SOCIETY
OF CHEMISTRY
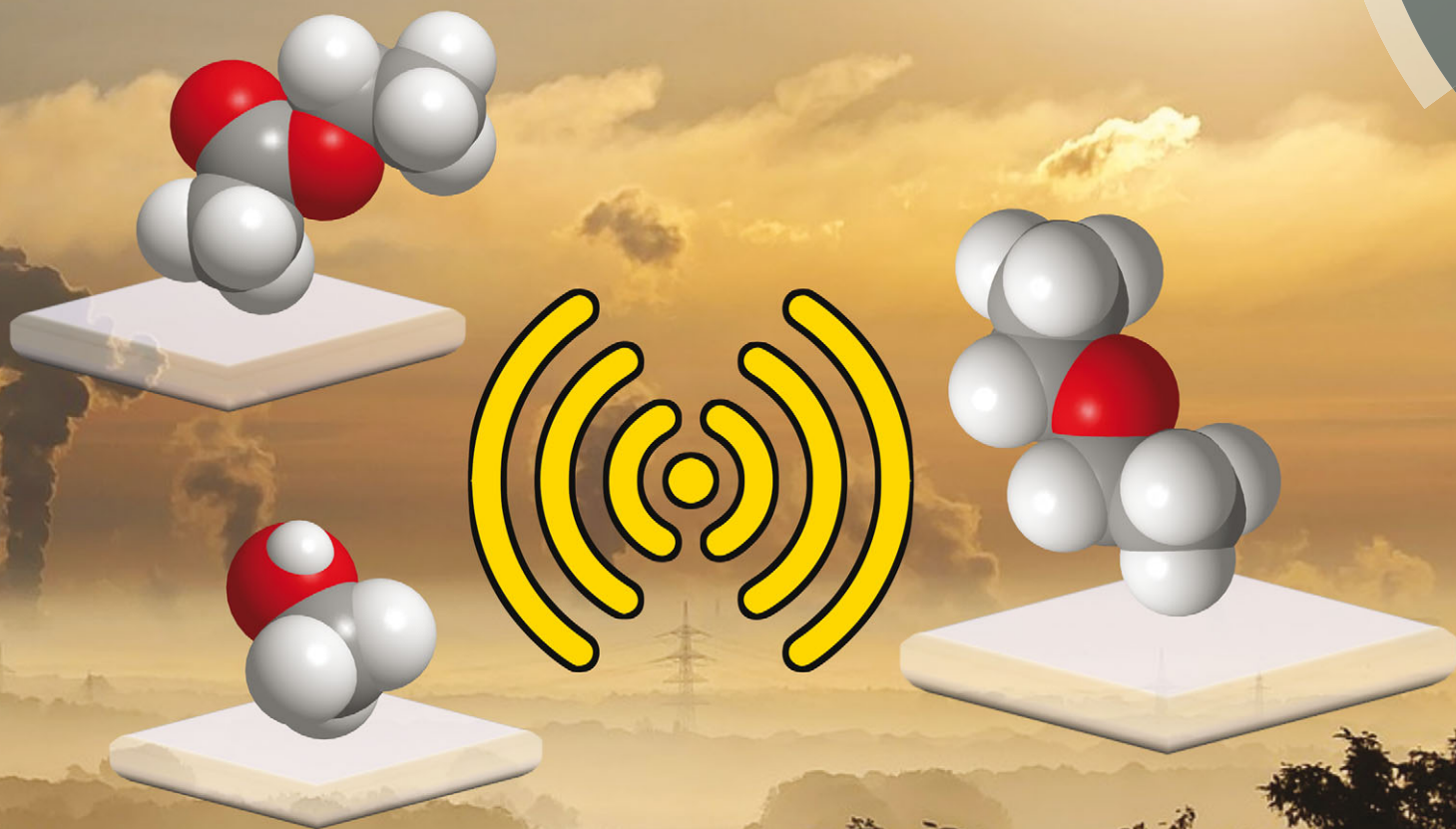
PAPER
J. C. Batchelor, S. J. Holder *et al.*
Swelling of PDMS networks in solvent vapours; applications for passive
RFID wireless sensors

Swelling of PDMS networks in solvent vapours; applications for passive RFID wireless sensors†

C. V. Rumens,[a] M. A. Ziai,[b] K. E. Belsey,[a] J. C. Batchelor*[b] and S. J. Holder*[a]

The relative degree of swelling of a poly(dimethylsiloxane) (PDMS) network in organic vapours is demonstrated to be related to the chemical and physical properties of the organic compounds. The swelling ratio, based on volume change, Q_V, is directly correlated with the Hansen solubility parameters, δ_d, δ_p and δ_h and the vapour pressures of the organic vapours employed. A practical use for such PDMS networks in combination with an understanding of the relationship is demonstrated by the use of PDMS as a mechanical actuator in a prototype wireless RFID passive sensor. The swelling of the PDMS displaces a feed loop resulting in an increase in transmitted power, at a fixed distance.

Introduction

The largest class of commercial inorganic polymers are the silicones (most typically polydimethylsiloxane based) and the inorganic nature of the materials confers many advantages over carbon based systems such as high thermal and oxidative stability, very low surface free energy, and high equilibrium and dynamic flexibility.[1–6] In particular the ability of polydimethylsiloxane materials to absorb both volatile and non-volatile organic compounds is well known. As a consequence of this property it is routinely used in analytical applications in particular as a matrix for sampling substances form the air, water and soil in particular in solid phase extraction (SPE) techniques.[6–9] A downside of SPE is that the absorption of compounds can lead to significant swelling, which can be detrimental in such applications. PDMS (silicone) materials are also increasingly used as the key components for microfluidic systems due to their general inertness, but again swelling by organic solvents can be detrimental to their application.[10,11] Whitesides *et al.* demonstrated that the extent of PDMS swelling in solvents is principally determined by the solubility of the solvent in PDMS and in particular the Hildebrand solubility parameters of the solvents and PDMS.[12]

In this manuscript we will demonstrate the relationship between the Hansen solubility parameters and the vapour pressures of organic solvents and the resulting degree of swelling of a network PDMS material. Furthermore even though the swelling of PDMS is commonly seen as a negative characteristic for many applications, it offers excellent opportunities as an actuating mechanism in sensor devices. In particular we will demonstrate that the swelling of PDMS by an organic vapour can be utilised as the actuating component in a wireless sensor.

Passive radio frequency identification (RFID) sensors are highly desirable as they are low cost, energy-efficient, wireless and lightweight. Passive RFID sensors have been developed and successfully used to either detect and/or monitor a range of analytes such as, temperature,[13] strain,[14] moisture,[15] and volatile organic compounds (VOC).[16] There has been much interest in developing passive RFID VOC sensors for a number of applications including; monitoring food quality in packaging[17] and homeland security.[18] The majority of gas and vapour sensors, wireless and non-wireless rely on the variation of electrical properties (conductance, capacitance and permittivity) of a material in response to an analyte as a sensing method.

Fiddes and Yan demonstrated an RFID tag array, which utilised carbon black/polymer composites integrated into conventional RFID tags.[19] As the carbon black/polymer composite swells in vapour, the distance between the carbon black changes resulting in a conductive change. The overall resistance of the tag changes, which causes a change in the signal frequency transmitted from the RFID tag to change. Each of the RFID tags has a different polymer as the sensing element, therefore producing a unique pattern of signals for each vapour. Nafion polymer electrolytes (co-polymer of tetrafluoroethylene and sulfonyl fluoride vinyl ether) have also been utilised in sensing vapours. Potyrailo and Morris coated conventional RFID tags with a thin layer of Nafion polymer electrolytes; the resistance and capacitance of this polymer layer changes in response to vapour absorption.[20]

[a] *Functional Materials Group, School of Physical Sciences, University of Kent, Canterbury, Kent, UK CT2 7NH. E-mail: S.J.Holder@kent.ac.uk*

[b] *School of Engineering and the Digital Arts, University of Kent, Canterbury, Kent, UK CT2 7NT. E-mail: J.C.Batchelor@kent.ac.uk*

This journal is © The Royal Society of Chemistry 2015

J. Mater. Chem. C, 2015, **3**, 10091–10098 | 10091

Chemicapacitor systems have also been used as vapour sensors and have previously utilised the known swelling of PDMS in chemical vapour. Polymer-based capacitor sensors detect organic vapours through the absorption of vapour by the polymer, which results in variation of the polymer's permittivity leading to an overall change in capacitance of the sensor.[21] However, the variance in the polymer's permittivity can be extremely subtle which has led to either the addition of highly conductive additives to PDMS[22] or to measure the change in both permittivity (dielectric) and deformation of the polymer to increase sensitivity.[23]

We present a simple, low cost, wireless RFID sensor design that does not rely on capacitance variance, but takes advantage of the large physical deformation of PDMS elastomers when exposed to vapours using a displacement sensor design. RFID displacement sensors have previously been used in structural health monitoring[24] in the place of using strain gauges. However, to our knowledge a displacement tag design has not been used in vapour sensing.

Experimental

Materials

Silanol-terminated polydimethylsiloxane (PDMS) (cSt 1000, M_w 26 000) was obtained from Fluorochem Ltd. Tin(II) 2-ethyl-hexanaoate (95%) and tetraethyl orthosilicate (99%) were purchased from Sigma Aldrich. All the above chemicals were used as received. Acetone (lab grade), acetonitrile (HPLC grade), butan-1-ol (analytical grade), chlorobenzene (analytical grade), diethyl ether (analytical grade), ethanol (analytical grade), ethyl acetate (analytical grade), hexane (lab grade), methanol (analytical grade), methylene dichloride (HPLC grade), pentan-1-ol (analytical grade), propan-2-ol (analytical grade), tetrahydrofuran (HPLC grade), toluene (HPLC grade) and xylene (mixture of isomers with meta-xylene as the predominant isomer determined via ^{1}H NMR) (analytical grade) were purchased from Fisher Scientific and used as received.

Synthesis of PDMS elastomers

Silanol-terminated PDMS (8.00 g, 3.08×10^{-4} mol), cross-linking agent tetraethyl orthosilicate (0.13 g, 6.24×10^{-4} mol) and catalyst tin(II) 2-ethylhexanoate (0.18 cm^3, 1 M solution in toluene) were speed-mixed at 3500 rpm for 90 seconds in total. The mixture was poured into square moulds and allowed to cure at room temperature for 2 hours before being placed into an oven at 60 °C overnight. Homogenous mixing of the elastomer components was achieved using a DAC 150FV2-K speedmixer and elastomers were formed in PTFE square moulds (mould width = 2 cm, length = 2 cm and height = 0.2 cm).

Swelling experiments

PDMS elastomers were placed in a saturated atmosphere of each solvent vapour for 72 hours. To achieve a saturated atmosphere, 25 cm^3 of each solvent was poured into the bottom of a dessicator (internal seal diameter of 10.1 cm). The circular perforated shelf was placed back into the dessicator with a PDMS elastomer in a petri dish placed on top. The dessicator

was sealed and at the end of 72 hours excess solvent was still present indicating a saturated atmosphere was achieved. The volume and weight of each PDMS elastomer was measured before and after solvent vapour exposure. To measure the extent of PDMS swelling, the volume swelling ratio (Q_V), defined as the ratio of the volume of swollen PDMS to its dry volume was calculated along with the weight swelling ratio (Q_W), defined as the ratio of the weight of swollen PDMS to its dry weight. The volume of the PDMS elastomers was measured using digital calipers (0–150 mm). PDMS swelling experiments for each solvent were performed three times in total.

Absorption rate

Absorption rates of the PDMS elastomers were performed by placing the elastomers into a dessicator (internal seal diameter of 15.2 cm) with 50 cm^3 of a chosen solvent for 24 hours. The PDMS elastomers were placed onto 1 mm square grid paper for scaling purposes and rather than the usual concave dessicator lid, a flat glass lid was used to seal the dessicator to ensure good visual of the elastomers. To measure the PDMS lateral swelling over 24 hours solvent vapour exposure, photographs of the PDMS elastomers were taken every 30 minutes from a height of 2.5 cm (distance between the dessicator lid and camera). ImageJ software was used to calculate the area of the elastomer from each photograph and the area swelling ratio (Q_A), defined as the ratio of the area of the swollen PDMS to its original area was calculated.

RFID tag design

A folded dipole antenna with an inductive feed loop was designed to provide an input impedance which conjugately matched the tag transponder ASIC (Application Specific Integrated Circuit) RFID silicon chip (Higgs3 RFID chip provided by Alien Technology). CST Microwave Studio EM simulation software was used to tune the sensor response to European UHF RFID frequency (865.6–867.6 MHz) for maximum power transfer between the feed loop and the ASIC. The reader power required to activate the sensor tag at distanced in the un-swollen state is given by:[25]

$$d \leq \lambda/4\pi \sqrt{\text{EIRP} \times G_{\text{tag}} \times \tau/P_{\text{th}}} \qquad (1)$$

where the transmitted power (EIRP) has a maximum of 2 W in Europe. Tag antenna gain G_{tag} and ASIC sensitivity P_{th} are fixed by the tag design and chip technology respectively and λ is the wavelength of the transmission signal (35 cm). The power transmission coefficient t between the tag antenna and transponder ASIC is variable according to:[26]

$$\tau = 4R_{\text{ic}}R_{\text{ant}} / |Z_{\text{ic}} + Z_{\text{ant}}|^2 \qquad (2)$$

where Z_{ic} & Z_{ant} are the port impedances of the transponder ASIC and the tag antenna respectively, while R_{ic} and R_{ant} are the real (resistive) parts. The relative position of the inductively coupled feed loop to the tag antenna affects both Z_{ant} and R_{ant}. As a consequence if read distance d is fixed, t and therefore the required transmit power are functions of the loop position,
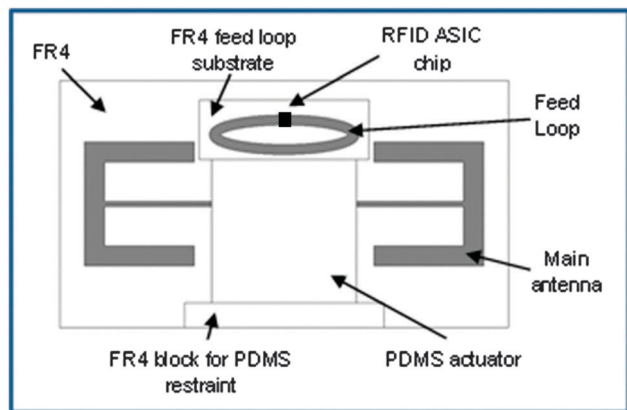
Fig. 1   Displacement feed loop RFID tag antenna.

with the power increasing as the loop moves away from the antenna.

The RFID tag design is shown in Fig. 1 and the tag dimensions are shown in Fig. S1 and Table S1 (ESI†). The main body of the antenna and feed loop were etched from two square pieces of 0.8 mm thick copper cladded FR4 (fibreglass reinforced epoxy laminate) circuit board. The RFID ASIC silicon chip (Higgs3 RFID chip provided by Alien Technology) was soldered across the slot in the feed loop and the PDMS elastomer was supported by an FR4 block to restrict its movement in that direction.

RFID measurements

The RFID tag was placed into a dessicator (internal seal diameter of 15.2 cm) with 50 cm³ of a chosen solvent. The dessicator was sealed with a flat glass lid. The dessicator was placed at a fixed distance, 30 cm above the RFID reader antenna. The tag read range was measured with a Voyantic Tagformance life RFID characterization system (Voyantic Ltd, Finland) which measures the backscattered power for the tag as a function of calibrated transmit power. Measurements were taken over a period of 24 hours solvent vapour exposure at 21 °C. For each measurement, the transmit power from the reader was ramped from 0–26.5 dBm over the frequency range, 800–1000 MHz. This transmit power value is then used to calculate tag read range according to eqn (1) for a calibrated system using a calibration tag with known parameters to determine the losses in the system. This transmit power value is then compared to that obtained from a standard tag with known parameters to determine the losses in the system using eqn (1). The transmitted power required to activate the tag relates directly to the coupling efficiency between the main body of the antenna and the feed loop, which decreases as the expanded PDMS elastomer forces the feed loop away from the main body of the antenna.

To describe RFID response we have calculated the transmitted power ratio, defined as the ratio of transmitted power (at 865 MHz) for the tag at a defined solvent vapour exposure time to the transmitted power (at 865 MHz) for 0 minute solvent vapour exposure.

Results and discussion

PDMS swelling

The PDMS elastomers were placed in a saturated atmosphere of each of the fifteen chosen solvent vapours for 72 hours, the long solvent exposure time was chosen to ensure the PDMS elastomers reached their maximum swelling. Fig. 2 shows the swelling ratio in terms of both weight and volume of the elastomers after vapour exposure. Each of the swelling experiments were performed a total of three times, the calculated standard errors (standard deviation of the mean) were small indicating our maximum swelling values of PDMS in each solvent vapour were reliable. Differences between Q_V and Q_W (Fig. 2) result from density differences between solvents (*i.e.* $Q_V > Q_W$ for densities <1 g ml^{-1} and $Q_V < Q_W$ for densities >1 g ml^{-1}) and the absolute degree of swelling (*i.e.* differences between Q_V and Q_W are greater for those solvents with densities furthest from 1 and that absorb more solvent). Thus dichloromethane, which shows good swelling and possesses a high density shows the largest difference between Q_W and Q_V. Furthermore few if any, of these PDMS-solvent systems are expected to show ideal 'solution' behaviour which will mean that volume changes upon mixing will occur.[27–29] A plot of the fractional difference between Q_V and Q_W with solvent densities is given in Fig. S9 (ESI†). The behaviour of all samples tested was reversible; after evaporation of the solvent from the PDMS the elastomers were observed to show identical swelling behaviour subsequently. However this was not tested extensively and currently forms the basis of ongoing research into tag design.

We have focused on using the volume swelling ratio in further analysis as our RFID tag antenna relies on the lateral deformation of the substrate. However all results have been analysed on the basis of weight and moles absorbed (see Table S2, ESI†) and
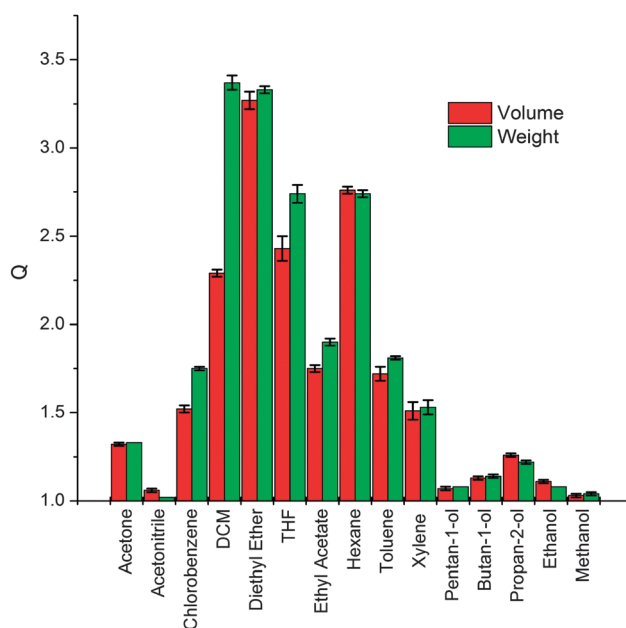

Fig. 2   Swelling ratio (Q) of PDMS elastomers after exposure to a range of solvent vapours.

This journal is © The Royal Society of Chemistry 2015

J. Mater. Chem. C, 2015, **3**, 10091–10098 | **10093**

no significant deviation in behaviour from that described in the main text was observed. Generally PDMS elastomers showed a degree of vapour specificity with non-polar to weakly polar solvent vapours with ethers (diethyl ether and tetrahydrofuran), hexane and DCM causing the largest swelling, ($Q_V > 2.0$) and polar solvent vapours, alcohols (pentan-1-ol, butan-1-ol, propan-2-ol, ethanol and methanol) and acetonitrile causing the least swelling ($Q_V = 1.0–1.3$) as might reasonably be expected for PDMS.

Correlation between swelling and solubility parameters

Previous research investigated PDMS swelling by the direct absorption of solvents (liquid–solid interface) found the extent of swelling could be correlated with the Hildebrand solubility parameter (δ, cal$^{1/2}$ cm$^{-3/2}$). In the Hildebrand model, solubility can be related to the cohesive energy of the molecule.[28,30]

$$\delta = (-E/V)^{1/2} \qquad (3)$$

where δ is the Hildebrand solubility parameter, $-E$ is the molecular cohesive energy and V is the molar volume. The cohesive energy of the molecule is derived from the heat of vaporisation. Solvents with a solubility parameter close to that of PDMS caused the largest swelling.[12] However, the authors did note a significant lack of correlation for certain solvents where those with similar solubility parameters caused significantly different degrees of PDMS swelling. The differences were attributed to the solvent polarity differences and the authors used the dipole moment of the solvent to explain the difference observed in swelling and represent the polar contributions to the overall solubility. Generally Hildebrand solubility parameters are good predictors for the compatibility of materials with non-polar and weakly polar solvents but are often poor for solvents with significant polar and/or hydrogen bonding properties.

As an extension of the Hildebrand method, Hansen suggested that the cohesive energy should be divided into three components: dispersion interactions (δ_d), dipolar interactions (δ_p) and hydrogen bonding interactions (δ_h).[31,32] These three components are known as the Hansen solubility parameters (MPa$^{1/2}$) and are additive:

$$\delta_t^2 = \delta_d^2 + \delta_p^2 + \delta_h^2 \qquad (4)$$

Solubility often follows the general rule of 'like dissolves like', for two materials to be soluble the Hansen solubility parameters of each material must be similar. In this manuscript, we will use Hansen solubility parameters (HSPs) over the Hildebrand solubility parameter. To measure the similarity of the HSP of PDMS to the HSP of each solvent, the Ra defined as the distance between the HSP's of two molecules was calculated for each solvent:[32,33]

$$Ra = \sqrt{4\left(\delta_{dp} - \delta_{ds}\right)^2 + \left(\delta_{pp} - \delta_{ps}\right)^2 + \left(\delta_{hp} - \delta_{hs}\right)^2} \qquad (5)$$

where p and s indicate the polymer and solvent contributions respectively. Thus the smaller the Ra value the higher the degree of absorption and the higher the swelling of PDMS. Fig. 3 shows the calculated values for each solvent versus the swelling ratio (Q_V). The Hansen solubility parameters and
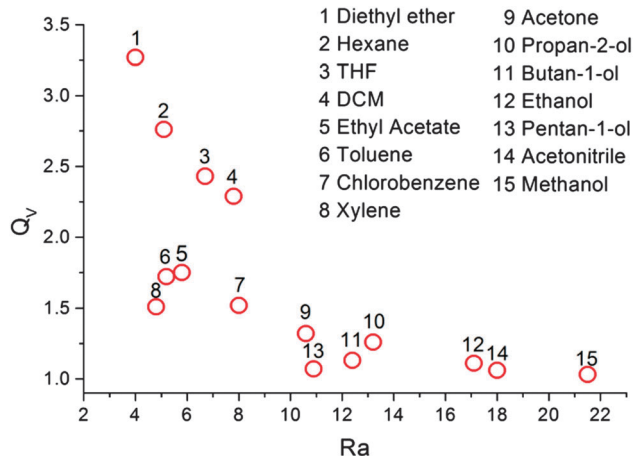

Fig. 3 Swelling ratio versus Ra for each solvent. The numbers relate to the ranking of the solvents swelling ability.

calculated Ra for each solvent can be found in Table S2 (ESI†). Solvents with an Ra < 8.0 show PDMS swelling, $Q_V > 1.5$ and solvents with an Ra > 8.0 show the least PDMS swelling $Q_V < 1.5$. However, there is no simple relationship between the value of Ra and the extent of PDMS swelling and whereas solvents with low polarities are ranked accurately in swelling ability the more polar solvents are not. The correlation coefficients for Q_V with δ_t and Ra were -0.76 and -0.60 respectively and thus whilst a correlation exists it is cannot based on solubility parameter alone.

Henry's Law states the overall absorbed concentration of gas, C (maximum PDMS swelling in this case) is directly proportional to the partial pressure of the gas, P and solubility, S.

$$C = SP \qquad (6)$$

A plot of Q_V versus vapour pressure (P_{vp}) was far from linear (Fig. S4(a), ESI†) but statistical analysis gave a strong correlation between the two properties (correlation coefficient = 0.73). Thus in accordance with Henry's law the relationship between both the total Hansen solubility parameter (δ_t), vapour pressure of the solvent and swelling ratio (Q_V) was plotted (Fig. 4). It was
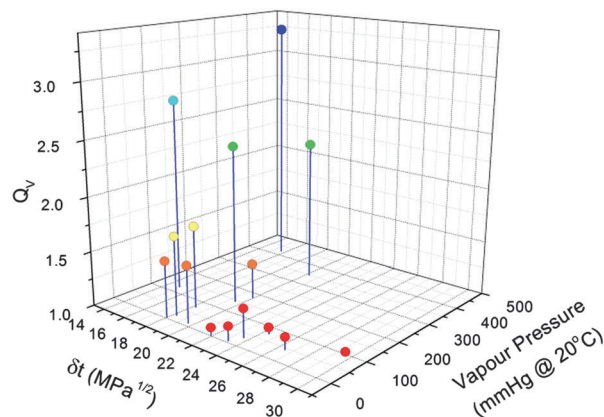

Fig. 4 Swelling ratio versus the total Hansen solubility parameter and vapour pressure of each solvent.

10094 | J. Mater. Chem. C, 2015, 3, 10091–10098

This journal is © The Royal Society of Chemistry 2015

observed that the difference in Q_V for solvents with similar total solubility parameters can be explained by the difference in the solvent's vapour pressures. Generally, a solvent with a high vapour pressure exhibits a larger Q_V than a solvent with a similar δ_t and a low vapour pressure. Linear regression analyses were performed using a range of x (independent) variables; including Hansen solubility parameters, Ra, vapour pressure, molar volume and water content. We used either the Hansen solubility parameters or Ra with various combinations of the other variables. The linear regression analyses were performed presuming that maximum PDMS swelling had been reached after 72 hours solvent vapour exposure.

Two sets of variables were found to produce the best linear fits; Ra and vapour pressure (eqn (7)) and the Hansen solubility parameters and vapour pressure (eqn (8)).

$$Q_V = a + b_{Ra} \times Ra + b_{P_{vp}} \times P_{vp} \qquad (7)$$

$$Q_V = a + (b_{\delta_d} \times \delta_d) + (b_{\delta_p} \times \delta_p) + (b_{\delta_h} \times \delta_h) + (b_{P_{vp}} \times P_{vp}) \qquad (8)$$

where a is the calculated intercept, b is the calculated slope from each independent variable, P_{vp} is the vapour pressure, δ_d is the dispersion solubility parameter, δ_p is the polarity solubility parameter and δ_h is the hydrogen bonding solubility parameter. The full results of the linear regression analysis can be found in Table S3 (ESI†). To ensure the association between the swelling ratio (Q_V) and each of the two sets of variables was statistically significant, the F-test for regression was performed at a confidence level of 95%. The F-test calculates the probability of the null hypothesis – in this case that the association between the swelling ratio and each of the two sets of variables is not statistically significant, that the fit was purely by chance. The F-test results as indicated by significance f in the linear regression output were all < 0.05 (significance f for eqn (5)$=3.34 \times 10^{-5}$ and eqn (6)$=9.984 \times 10^{-5}$). The small significance f calculated led to the rejection of the null hypothesis and therefore confirmed the validity of the linear fit. Further significance f results for Q_W can be found in Table S3 (ESI†).

The predicted Q_V values calculated using eqn (6) were plotted against our measured values of Q_V as shown in Fig. 5.
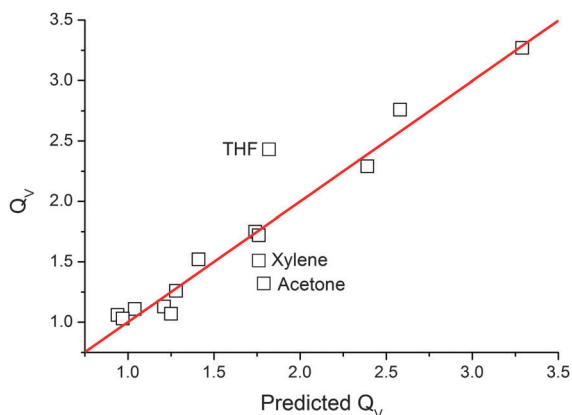

Fig. 5 Measured volume swelling ratio *versus* predicted swelling ratio calculated using eqn (6).

This predicted-measured plot was used to visually assess the prediction error for each of the predicted values and therefore how well the linear regression model fitted the data. A few outliers (deviations from the line) were noted, with the largest deviation from the line being THF and the other smaller two outliers being xylene and acetone. However, we found the linear regression model was a good fit as the majority of the predictions laid close to or directly on the linear fit line. This relationship enables us to gauge the extent of PDMS swelling by other solvent vapours.

Vapour absorption rate/diffusion

Absorption rate experiments were performed in 6 solvent vapours; 2 vapours that caused large PDMS swelling (diethyl ether and DCM), 2 vapours which caused mid-range PDMS swelling (acetone and xylene) and 2 vapours that caused small PDMS swelling (methanol and acetonitrile). To prevent continually removing the PDMS elastomers from the saturated vapour atmosphere for measurements, the area of the elastomer was measured rather than the volume. Fig. 6(c) shows the relationship between PDMS area swelling, Q_A and solvent vapour exposure time over a period of 24 hours. The curves best fit was achieved using a 2-phase exponential association model:

$$Q_V = Q_{V_o} + A_1\left(1 - e^{-\frac{t}{t1}}\right) + A_2\left(1 - e^{-\frac{t}{t2}}\right) \qquad (9)$$

The model enabled us to predict the maximum area swelling of the PDMS elastomers in the six chosen vapours. The maximum Q_A was used to investigate the swelling kinetics of PDMS. In diethyl ether, DCM, acetone, acetonitrile, methanol and xylene solvent vapour, PDMS had reached 97.6%, 95.2%, 95.0%, 100%, 100% and 69.7% maximum swelling respectively after 24 hours exposure. In all the solvent vapours apart from xylene, PDMS had almost reached maximum swelling after 24 hours, confirming our assumption previously that after 72 hours maximum PDMS swelling should have been achieved. One possible reason for PDMS reaching a smaller percentage of its maximum swelling in xylene compared to other solvent vapours is xylene's large molar volume of 123.4 and low vapour pressure. The molecular size of the vapour (the diffusant) can affect diffusion – the larger the diffusant, the longer it takes for equilibrium (maximum swelling) to be reached.[34] Diffusion of vapours and gases into polymers occurs by random molecular motion to equalise the concentration difference or remove the chemical potential difference between the diffusant and polymer.

Many diffusion processes through elastomeric polymers can be described by Fick's first law of diffusion:[35]

$$J = -D(\delta_c/\delta_x) \qquad (10)$$

where the flux, J is directly proportional to the concentration gradient (δ_c/δ_x) and D is the diffusion coefficient. The swelling kinetics of PDMS in diethyl ether, DCM and xylene vapour is shown in Fig. 7.‡ The first 55% of swelling by all three solvent

---

‡ The plots obtained for acetonitrile, acetone and methanol could not be reliably used for this analysis due to either a limited number of data points in the initial swelling region and/or too high a degree of error associated with the measurement of area increase.
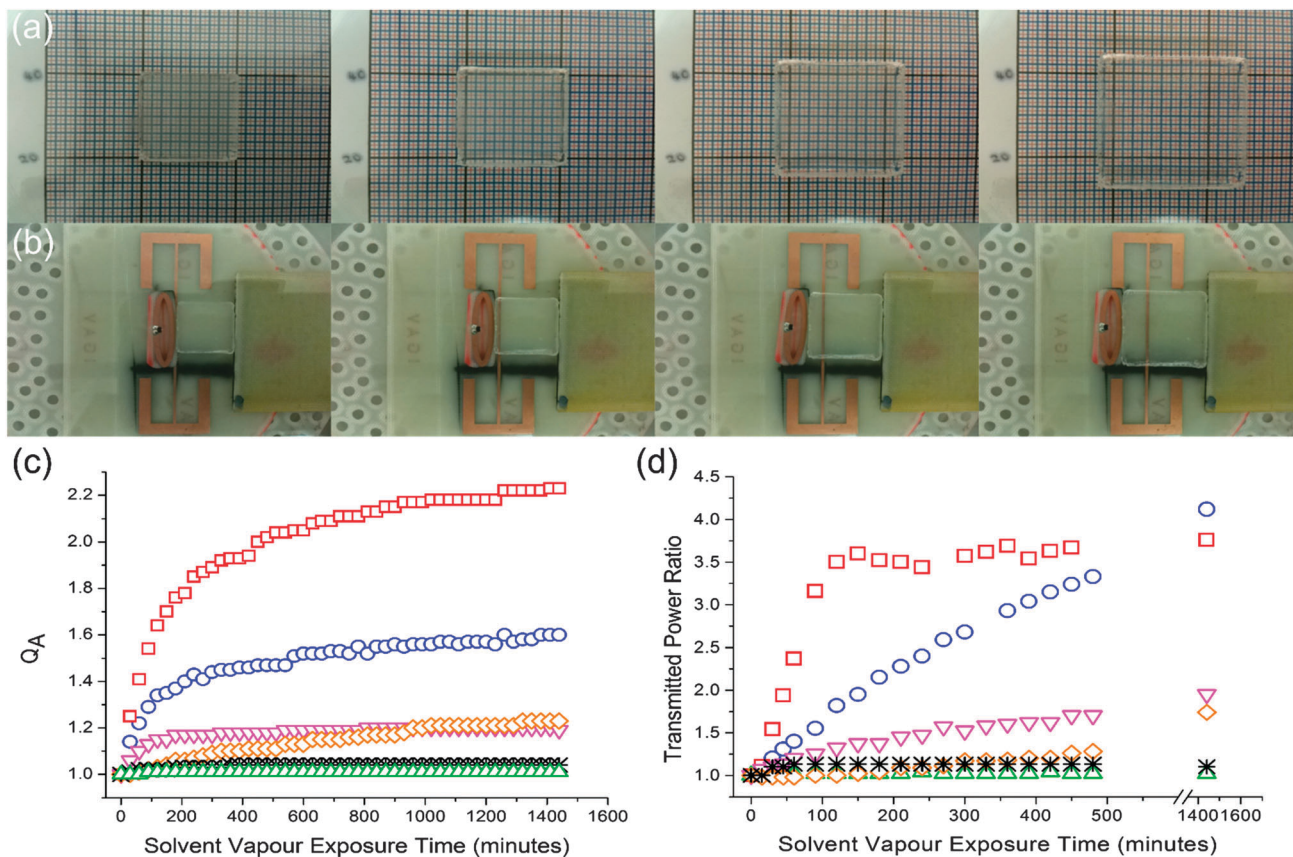
This journal is © The Royal Society of Chemistry 2015

J. Mater. Chem. C, 2015, **3**, 10091–10098 | **10095**

Fig. 6 (a) Image of an elastomer from left to right after 0 minutes, 30 minutes, 150 minutes and 1440 minutes diethyl ether vapour exposure: top – images taken during absorption rate measurements. (b) Images taken during RFID measurements. (c) Area swelling ratio *versus* solvent exposure time. (d) Transmitted power ratio *versus* the solvent vapour exposure time. The symbols representing different solvents are the same for both (c) and (d) where: □ diethyl ether, ○ DCM, ▽ acetone, ◇ xylene, △ methanol and * acetonitrile.

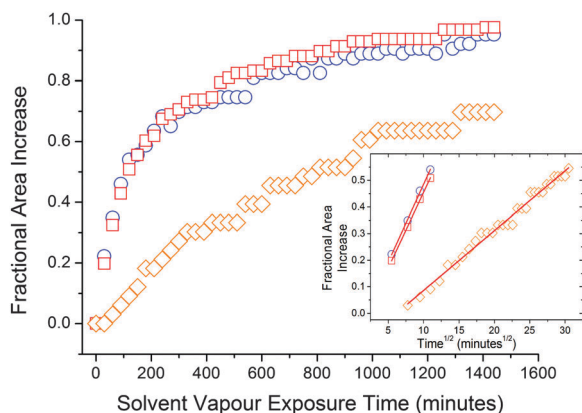**Fig. 7** Swelling kinetics for PDMS in □ diethyl ether, ○ DCM and ◇ xylene. Inset figure shows the first 55% swelling data *versus* the square root of time.

vapours (Fig. 7 inset) displayed a linear relationship associated with Fickian diffusion.[36] This linear relationship further suggests case 1 Fickian diffusion where the mobility of the diffusant is slower than the polymer chain mobility.[37] In this case, the diffusion of vapours into PDMS is mostly governed by the properties of the diffusant (*i.e.* physical state and molecular

size) rather than the properties of the PDMS elastomer (*i.e.* morphology of the polymer). The slope of fractional area with the square root of time can be taken as equivalent to the diffusion coefficient. As noted previously the diffusion coefficients of diethyl ether and DCM in PDMS are larger than the diffusion coefficient of xylene in PDMS.

RFID measurements

RFID measurements were performed using six solvents in total: 2 high swelling solvents (diethyl ether and methylene dichloride), 2 middle swelling solvents (xylene and acetone) and 2 least swelling solvents (acetonitrile and methanol). The tag transmitted power was measured for 24 hours. Transmitted power (dBm) is the output energy from the RFID reader required to turn on the passive RFID tag. As the loop moves further away from the main antenna, the required power needed to power the RFID tag increases. Transmitted power ratio *versus* solvent vapour exposure time is shown in Fig. 6(d). Our RFID sensor is able to differentiate between solvent vapours as demonstrated by the varying magnitude of RFID response to each solvent vapour. As expected, the solvents that caused the largest PDMS swelling caused the largest increase in transmitted power and hence sensor response. The RFID sensor is limited by the

distance displaced by the loop antenna; this is clearly seen by the plateau exhibited after 150 minutes of diethyl ether vapour exposure in Fig. 6(d). Once the tag requires around 3.5 times more power than the minimum it requires, the tag becomes less sensitive and can no longer monitor vapour exposure. RFID response is proportional to the degree of PDMS swelling at a particular time of solvent vapour exposure, and therefore the general identity of the organic vapour. Further tag design will enable reversibility to be built into the displacement arrangement.

Conclusions

We have demonstrated that the swelling ratio of a PDMS network, based on volume change, Q_V, can be directly correlated with the Hansen solubility parameters, δ_d, δ_p and δ_h and the vapour pressures of the organic vapours employed. That the relative degree of swelling of a PDMS network in organic vapours is dependent upon the chemical and physical properties of the organic vapours in question is not surprising. Henry's law when applied to polymers has been known to relate concentration of gas absorbed to pressure and the solubility coefficient has been known for decades. However the use of Hansen solubility parameters as a guide to solubility in combination with vapour pressure (in this instance) allows for an easy guide to predict relative swelling of a polymer by a range of solvent vapours.

We demonstrate a practical use for such PDMS networks in combination with an understanding of the relationship, is by using PDMS as a mechanical actuator in a prototype wireless RFID passive sensor. The swelling of the PDMS displaces a feed loop in the RFID sensor resulting in an increase in transmitted power, at a fixed distance.

Whilst the PDMS is not chemically specific in its absorption capability it shows a preference for non-polar and weakly polar solvents. In future work we will enable higher degrees of chemical specificity by introducing threshold limits into the sensor design (*i.e.* distance of actuator from the displacement component). Furthermore the polysiloxane component is highly amenable to chemical functionalization and a range of commercial polysiloxanes are available that retain high permeability but display different solubility parameters. The reversibility of the PDMS swelling will enable reversible wireless vapour sensing by future modification of the tag design. Future sensor design will use significantly smaller components through the use of printed antenna and smaller PDMS samples with differing solubility characteristics.

Acknowledgements

Notes and references

1 F. Abbasi, H. Mirzadeh and A. Katbab, *Polym. Int.*, 2001, **50**, 1279–1287.

2 S. J. Clarson, in *Silicon-Containing Polymers*, ed. R. G. Jones, W. Ando and J. Chojnowski, Springer, 2000, pp. 139–155.

3 P. R. Dvornic and R. W. Lenz, *High Temperature Siloxane Elastomers*, Wepf, 1990.

4 D. Graiver and G. Fearon, in *Silicon-Containing Polymers*, ed. R. G. Jones, W. Ando and J. Chojnowski, Springer, 2000, pp. 233–243.

5 J. E. Mark, *Acc. Chem. Res.*, 2004, **37**, 946–953.

6 S. Seethapathy and T. Górecki, *Anal. Chim. Acta*, 2012, **750**, 48–62.

7 S. Balasubramanian and S. Panigrahi, *Food Bioprocess Technol.*, 2011, **4**, 1–26.

8 H. Kataoka, *Anal. Sci.*, 2011, **27**, 893.

9 A. Spietelun, M. Pilarczyk, A. Kloskowski and J. Namieśnik, *Chem. Soc. Rev.*, 2010, **39**, 4524–4537.

10 Y. Huang, K. Choi and C. H. Hidrovo, *Microelectron. Eng.*, 2014, **124**, 66–75.

11 B. Kim, L. Hong, Y. Chung, D. Kim and C. Lee, *Adv. Funct. Mater.*, 2009, **19**, 3796–3803.

12 J. N. Lee, C. Park and G. M. Whitesides, *Anal. Chem.*, 2003, **75**, 6544–6554.

13 J. Virtanen, F. Yang, L. Ukkonen, A. Elsherbeni, A. Babar and L. Sydänheimo, *Sens. Rev.*, 2014, **34**, 154–169.

14 O. O. Rakibet, C. V. Rumens, J. C. Batchelor and S. J. Holder, *IEEE Antenn. Wirel. Pr.*, 2014, **13**, 814–817.

15 A. Oprea, N. Barsan, U. Weimar, M. Bauersfeld, D. Ebling and J. Wöllenstein, *Sens. Actuators, B*, 2008, **132**, 404–410.

16 R. A. Potyrailo, A. Burns, C. Surman, D. Lee and E. McGinniss, *Analyst*, 2012, **137**, 2777–2781.

17 R. A. Potyrailo, N. Nagraj, Z. Tang, F. J. Mondello, C. Surman and W. Morris, *J. Agric. Food Chem.*, 2012, **60**, 8535–8543.

18 R. A. Potyrailo, N. Nagraj, C. Surman, H. Boudries, H. Lai, J. M. Slocik, N. Kelley-Loughnane and R. R. Naik, *TrAC, Trends Anal. Chem.*, 2012, **40**, 133–145.

19 L. K. Fiddes and N. Yan, *Sens. Actuators, B*, 2013, **186**, 817–823.

20 R. A. Potyrailo and W. G. Morris, *Anal. Chem.*, 2007, **79**, 45–51.

21 S. Patel, T. Mlsna, B. Fruhberger, E. Klaassen, S. Cemalovic and D. Baselt, *Sens. Actuators, B*, 2003, **96**, 541–553.

22 S. Dissanayake, C. Vanlangenberg, S. V. Patel and T. Mlsna, *Sens. Actuators, B*, 2015, **206**, 548–554.

23 U. Altenberend, A. Oprea, N. Barsan and U. Weimar, *Anal. Bioanal. Chem.*, 2013, **405**, 6445–6452.

24 M. J. Cazeca, J. Mead, J. Chen and R. Nagarajan, *Sens. Actuators, A*, 2013, **190**, 197–202.

25 K. Finkenzeller, *RFID Handbook*, John Wiley & Sons, Ltd, 2010, pp. 61–154.

26 K. V. S. Rao, P. V. Nikitin and S. F. Lam, *Automatic Identification Advanced Technologies, 2005. Fourth IEEE Workshop on, IEEE*, 2005, pp. 39–42.

27 A. F. Barton, *Handbook of Polymer-Liquid Interaction Parameters and Solubility Parameters*, CRC press, 1990.

28 A. F. Barton, *Chem. Rev.*, 1975, **75**, 731–753.

29 I. C. Sanchez and R. H. Lacombe, *Macromolecules*, 1978, **11**, 1145–1156.

This journal is © The Royal Society of Chemistry 2015

J. Mater. Chem. C, 2015, **3**, 10091–10098 | 10097

30 H. A. Benesi and J. Hildebrand, *J. Am. Chem. Soc.*, 1949, **71**, 2703–2707.

31 C. M. Hansen, *Prog. Org. Coat.*, 2004, **51**, 77–84.

32 C. M. Hansen, *Hansen Solubility Parameters: A User's Handbook*, CRC press, 2007.

33 T. Lindvig, M. L. Michelsen and G. M. Kontogeorgis, *Fluid Phase Equilib.*, 2002, **203**, 247–260.

34 M. Saleem, A. A. Asfour, D. De Kee and B. Harrison, *J. Appl. Polym. Sci.*, 1989, **37**, 617–625.

35 S. C. George and S. Thomas, *Prog. Polym. Sci.*, 2001, **26**, 985–1017.

36 P. K. Chatterjee and B. S. Gupta, *Text. Sci. Technol.*, 2002, **13**, 1–55.

37 L. Masaro and X. Zhu, *Prog. Polym. Sci.*, 1999, **24**, 731–775.

10098 | *J. Mater. Chem. C,* 2015, **3**, 10091–10098

This journal is © The Royal Society of Chemistry 2015